Langmuir
Article
pubs.acs.org/Langmuir
© 2010 American Chemical Society

Enzyme:Nanoparticle Bioconjugates with Two Sequential Enzymes: Stoichiometry and Activity of Malate Dehydrogenase and Citrate Synthase on Au Nanoparticles

Jacqueline D. Keighron and Christine D. Keating*

Department of Chemistry, The Pennsylvania State University, University Park, Pennsylvania 16802, United States

Received October 11, 2010. Revised Manuscript Received November 8, 2010

We report the synthesis and characterization of bioconjugates in which the enzymes malate dehydrogenase (MDH) and/or citrate synthase (CS) were adsorbed to 30 nm diameter Au nanoparticles. Enzyme:Au stoichiometry and kinetic parameters (specific activity, k_{cat}, K_M, and activity per particle) were determined for MDH:Au, CS:Au, and three types of dual-activity MDH/CS:Au bioconjugates. For single-activity bioconjugates (MDH:Au and CS:Au), the number of enzyme molecules adsorbed per particle was dependent upon the enzyme concentration in solution, with multilayers forming at high enzyme:Au solution ratios. The specific activity of adsorbed enzyme increased with increasing number adsorbed per particle for CS:Au, but was less sensitive to stoichiometry for MDH:Au. Dual activity bioconjugates were prepared in three ways: (1) by adsorption of MDH followed by CS, (2) by adsorption of CS followed by MDH, and (3) by coadsorption of both enzymes from the same solution. The resulting bioconjugates differed substantially in the number of enzyme molecules adsorbed per particle, the specific activity of the adsorbed enzymes, and also the enzymatic activity per particle. Bioconjugates formed by adding CS to the Au nanoparticles before MDH was added exhibited higher specific activities for both enzymes than those formed by adding the enzymes in the reverse order. These bioconjugates also had 3-fold higher per-particle sequential activity for conversion of malate to citrate, despite substantially fewer copies of both enzymes present.

Introduction

Biomolecule−nanoparticle conjugates are increasingly important in a wide range of applications including bioanalysis, imaging, and medicine. In particular protein−nanoparticle bioconjugates have been used as electron-dense biospecific stains in electron microscopy for many years and more recently are showing promise for applications such as bioanalysis, biocatalysis, and nanomedicine.[1−5] For example, antibody-coated particles have been used as affinity labels to detect antigens via changes in solution optical absorbance or scattering, surface plasmon resonance, surface enhanced Raman scattering, or electrical conductivity.[3] Enzyme-nanoparticle conjugates that take advantage of the catalytic ability of bound enzymes have been reported for bioanalytical and biotechnological applications.[1,2,6] Increasingly complex multienzyme conjugates are being developed.[7−9] For example, the sequential enzymes horseradish peroxidase (HRP) and glucose oxidase (GOx) have been coimmobilized in polyelectrolyte multilayers on silica microparticles.[8] A set of three sequential enzymes was immobilized on phospholipid polymer particles to facilitate the overall reaction.[9] Multiactivity bioconjugates such as these are attractive as model systems for biological enzyme assemblies, in bioanalytical sensors, and for industrial processes.[8−12] For any of these applications, the performance of the final constructs is impacted by a number of different factors, and, consequently, characterization of the conjugates, and in particular their enzymatic activity, is essential.

Many methods have been reported for preparation of protein−nanoparticle conjugates.[4] Electrostatic attraction can be used to assemble proteins in polyelectrolyte multilayers.[13,14] Reactive functional groups such as primary amines, thiols, or carboxylates present on the protein can be coupled to molecules on the particle surface using any number of cross-linking chemistries.[15,16] Depending on the presence and distribution of the reactive groups, chemical

*To whom correspondence should be addressed. E-mail: keating@chem.psu.edu.

(1) (a) Willner, I.; Basnar, B.; Willner, B. Nanoparticle−enzyme hybrid systems for nanobiotechnology. *FEBS J.* **2007**, *274*, 302–309. (b) Willner, I.; Baron, R.; Willner, B. Integrated nanoparticle−biomolecule systems for biosensing and bioelectronics. *Biosens. Bioelectron.* **2007**, *22*, 1841–1852.

(2) Hayat, M. A. *Colloidal Gold Principles, Methods, and Applications*; Academic Pres, Inc.: San Diego, CA, 1989; Vol. *1*−*3*.

(3) Katz, E.; Willner, I. Integrated nanoparticle-biomolecule hybrid systems: Synthesis, properties, and applications. *Angew. Chem., Int. Ed.* **2004**, *43*, 6042–6108.

(4) Niemeyer, C. M. Nanoparticles, proteins, and nucleic acids: Biotechnology meets materials science. *Angew. Chem., Int. Ed.* **2001**, *40*, 4128–4158.

(5) Rosi, N. L.; Mirkin, C. A. Nanostructures in biodiagnostics. *Chem. Rev.* **2005**, *105*, 1547–1562.

(6) (a) Kreft, O.; Prevot, M.; Mohwald, H.; Sukhorukov, G. Shell-in-shell microcapsules: A novel tool for integrated, spatially confined enzymatic reactions. *Angw. Chem. Int. Ed.* **2007**, *46*, 5605–5608. (b) Wiemann, L. O.; Buthe, A.; Klein, M.; van den Wittenboer, A.; Dahne, L.; Ansorge-Schumacher, M. B. Encapsulation of synthetically valuable biocatalysts into polylelectrolyte multilayer systems. *Langmuir* **2009**, *25*, 618–623.

(7) Caruso, F.; Fiedler, H.; Haage, K. Assembly of β-glucosidase multilayers on spherical colloidal particles and their use as active catalysts. *Colloids Surf., A* **2000**, *169*, 287–293.

(8) Pescador, P.; Katakis, I.; Toca-Herrera, J. L.; Donath, E. Efficiency of a bienzyme sequential reaction system immobilized on polyelectrolyte multilayer-coated colloids. *Langmuir* **2008**, *24*, 14108–14114.

(9) Watanabe, J.; Ishihara, K. Sequential enzymatic reactions and stability of biomolecules immobilized onto phospholipid polymer nanoparticles. *Biomacromolecules* **2006**, *7*, 171–175.

(10) Kuhn, S. J.; Finch, S. K.; Hallahan, D. E.; Giorgio, T. D. Facile production of multivalent enzyme−nanoparticle conjugates. *J. Magn. Magn. Mater.* **2007**, *311*, 68–72.

(11) Dai, Z. H.; Bao, H. C.; Yang, X. D.; Ju, H. X. A bienzyme channeling glucose sensor with a wide concentration range based on co-entrapment of enzymes in SBA-15 mesopores. *Biosens. Bioelectron.* **2008**, *23*, 1070–1076.

(12) Muller, J.; Niemeyer, C. M. DNA-directed assembly of artificial multienzyme complexes. *Biochem. Biophys. Res. Commun.* **2008**, *377*, 62–67.

(13) Caruso, F.; Schuler, C. Enzyme multilayers on colloid particles: Assembly, stability, and enzymatic activity. *Langmuir* **2000**, *16*, 9595–9603.

(14) Ariga, K.; Hill, J. P.; Ji, Q. M. Layer-by-layer assembly as a versatile bottom-up nanofabrication technique for exploratory research and realistic application. *Phys. Chem. Chem. Phys.* **2007**, *9*, 2319–2340.

(15) Hermanson, G. T. *Bioconjugate Techniques.*; Academic Press: San Diego, CA, 1996.

(16) Rusmini, F.; Zhong, Z.; Feigen, J. Protein immobilization strategies for protein biochips. *Biomacromolecules* **2007**, *8*, 1775–1789.

coupling can result in excellent to very poor retention of bioactivity for bound proteins. Alternatively, the techniques of molecular biology can be used to insert unique functional groups (e.g., cysteine residues, C- or N-terminal polyhistidine tags) at predetermined sites to enable oriented attachment. This approach requires greater effort, but provides excellent control over the properties of the resulting bioconjugates.[17] For example, Abad and co-workers showed nearly 100% activity retention for histidine-tagged HRP conjugation to Co(II)-nitrilotriacetic acid-functionalized gold particles.[18] Despite these successes, the most commonly used means of bioconjugation is direct adsorption, where nanoparticles are simply exposed to the protein in solution, and the resulting conjugates are separated by centrifugation. Proteins adhere nonspecifically to the particle surface through a combination of hydrogen bonding, hydrophobic, van der Waals, and/or electrostatic interactions.[19,20] Enzyme adsorption often results in a significant loss of catalytic activity due to denaturation and/or blockage of the active site.[19−25] After an initial activity loss, however, particle-bound enzymes have in several cases been shown to resist further activity loss upon aging, pH changes, or exposure to high temperatures better than free enzyme.[25−27]

Because enzyme structure, active site accessibility, and/or catalytic activity have been shown to change upon adsorption for many enzyme−nanoparticle systems, it is important to characterize nanobioconjugates. Enzymatic activity and Michaelis−Menten kinetics parameters for bioconjugates vary widely depending on the enzyme, the size and type of nanoparticle, and the conjugation method.[25,26,28,29] Circular dichroism spectroscopy and tryptophan fluorescence have provided information on enzyme secondary structure[19,25,30−32] and, when coupled with activity measurements, can lend insight into whether conformational changes or active site orientation are responsible for observed changes in activity as compared to free enzymes.[22−24] In many cases, the number of enzyme molecules bound to each nanoparticle and/or the total number of nanoparticles in solution are not known. Consequently, reports of specific activity are relatively uncommon,[21] particularly for multienzyme conjugates. Specific activity, measured as U/mg of enzyme, is a standard measurement for determining enzyme purity.[33] For enzyme−nanoparticle conjugates, it can give the extent of inactivation due to the combined effects of denaturation, orientation, and steric hindrance.

Scheme 1. Multienzyme Bioconjugates Prepared by Sequential or Simultaneous Addition of MDH and CS[34]

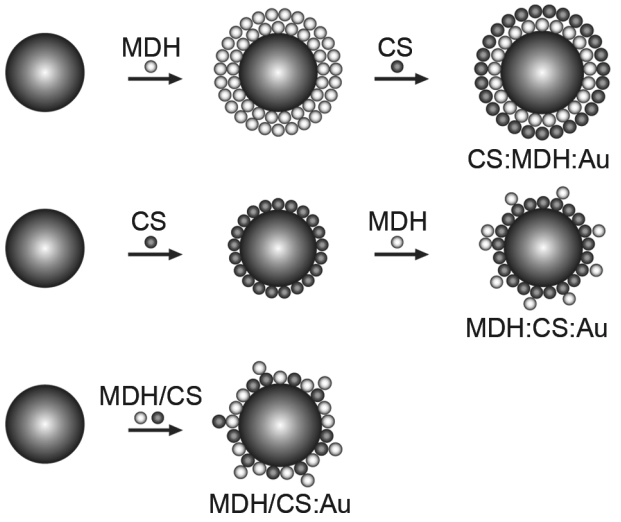

In this manuscript, we describe the preparation and characterization of enzyme:Au nanoparticle (Au NP) bioconjugates incorporating two different enzymes: malate dehydrogenase (MDH) and citrate synthase (CS). Bioconjugates were prepared by direct adsorption of one or both enzymes to 30-nm diameter gold nanospheres as illustrated in Scheme 1. The two enzymes were labeled with different fluorescent dyes, which made it possible to quantify the number of copies of each enzyme adsorbed per nanoparticle and determine specific activities for bound versus free enzyme. Substrate saturation (K_M), turnover number (k_{cat}), and per-particle individual and sequential activities were also determined. By varying the order in which enzymes were adsorbed, we were able to investigate the effect of each enzyme on the adsorption and activity of the other. In all cases, we observed a decrease in specific activity upon adsorption for both enzymes, suggesting structural perturbations and/or decreased accessibility of the active sites. However, both the number of copies each enzyme bound and their specific activities depended on the order of addition of the enzymes to the nanoparticles. The specific activity of MDH and CS varied by nearly an order of magnitude in different configurations on the surface.

Results and Discussion

We chose for this study two well-characterized, readily available enzymes that carry out a sequential reaction (Scheme 2) as

(17) (a) Turkova, J. Oriented immoblization of biologically active proteins as a tool for revealing protein interactions and function. *J. Chromatogr. B* **1999**, *722*, 11–31. (b) Stayton, P. S.; Olinger, J. M.; Jiang, M.; Bohn, P. W.; Sligar, S. G. Genetic-engineering of surface attachment sites yields oriented protein monolayers. *J. Am. Chem. Soc.* **1992**, *114*, 9298–9299. (c) McLean, M. A.; Stayton, P. S.; Sligar, S. G. Engineeriing protein orientation at surfaces to control molecular recognition events. *Anal. Chem.* **1993**, *65*, 2676–2678. (d) Huang, W.; Wang, J. Q.; Bhattacharyya, D.; Bachas, L. G. Improving the activity of immobilized subtilisin by site-specific attachment to surfaces. *Anal. Chem.* **1997**, *69*, 4601–4607.

(18) Abad, J. M.; Mertens, S. F. L.; Pita, M.; Fernandez, V. M.; Schiffrin, D. J. Functionalization of thioctic acid-capped gold nanoparticles for specific immobilization of histidine-tagged proteins. *J. Am. Chem. Soc.* **2005**, *27*, 5689–5694.

(19) Vertegal, A. A.; Siegel, R. W.; Dordick, J. S. Silica nanoparticle size influences the structure and enzymatic activity of adsorbed lysozyme. *Langmuir* **2004**, *20*, 6800–6807.

(20) Malmsten, M. Protein adsorption at the solid-liquid interface. In *Protein Architecture: Interfacing Molecular Assemblies and Immobilization Biotechnology*. Lvov, Y.; Mohwald, H., Eds.; Marcel Dekker: New York, 2000.

(21) Cans, A.-S.; Dean, S. L.; Reyes, F. E.; Keating, C. D. Synthesis and characterization of enzyme-Au bioconjugates: HRP and fluorescein-labeled HRP. *NanoBiotechnology* **2007**, *3*, 12–22.

(22) Sivaraman, B.; Fears, K. P.; Latour, R. A. Investigation of the effects of surface chemistry and solution concentration on the conformation of adsorbed proteins using an improved circular dichroism Method. *Langmuir* **2009**, *25*, 3050–3056.

(23) Fears, K. P.; Sivaraman, B.; Powell, G. L.; Wu, Y.; Latour, R. A. Probing the conformation and orientation of adsorbed enzymes using side-chain modification. *Langmuir* **2009**, *25*, 9319–9327.

(24) Fears, K. P.; Latour, R. A. Assessing the influence of adsorbed-state conformation on the bioactivity of adsorbed enzyme layers. *Langmuir* **2009**, *25*, 13926–13933.

(25) Pandey, P.; Singh, S. P.; Arya, S. K.; Gupta, V.; Datta, M.; Singh, S.; Malhotra, B. D. Application of thiolated gold nanoparticles for the enhancement of glucose oxidase activity. *Langmuir* **2007**, *23*, 3333–3337.

(26) Sharma, A.; Qiang, Y.; Antony, J.; Meyer, D.; Kornacki, P.; Paszczynski, A. Dramatic increase in stability and longevity of enzymes attached to monodispersive iron nanoparticles. *IEEE Trans. Magn.* **2007**, *43*, 2418–2420.

(27) Kouassi, G. K.; Irudayaraj, J.; McCarty, G. Examination of Cholesterol oxidase attachment to magnetic nanoparticles. *J. Nanobiotechnol.* **2005**, *3*, 1–9.

(28) Dykman, L. A.; Bogatyrev, V. A.; Khlebtsov, B. N.; Khlebtov, N. G. A protein assay based on colloidal gold conjugates with trypsin. *Anal. Biochem.* **2005**, *341*, 16–21.

(29) Huang, S.-H.; Liao, M.-H.; Chen, D.-H. Direct binding and characterization of lipase onto magnetic nanoparticles. *Biotechnol. Prog.* **2003**, *19*, 1095–1100.

(30) Aubin-Tam, M.-E.; Zhou, H.; Hamad-Schifferli, K. Structure of cytochrome c at the interface with magnetic $CoFe_2O_4$ nanoparticles. *Soft Matter* **2008**, *4*, 554–559.

(31) Priyam, A.; Chatterjee, A.; Bhattacharya, S. C.; Saha, A. Conformation and activity dependent interactions of glucose oxidase with CdTe quantum dots: Towards developing a nanoparticle based enzymatic assay. *Photochem. Photobiol. Sci.* **2009**, *8*, 362–370.

(32) Gole, A.; Dash, C.; Soman, C.; Sainkar, S. R.; Rao, M.; Sastry, M. On the preparation, characterization, and enzymatic activity of fungal protease−gold colloid bioconjugates. *Bioconjugate Chem.* **2001**, *12*, 684–690.

(33) Berg, J. M.; Tymoczko, J. L.; Stryer, L. *Biochemistry*, 6th ed.; W. H. Freeman and Company: New York, 2007.

Scheme 2. Enzymatic Reactions Carried out by MDH and CS Individually and in Sequence

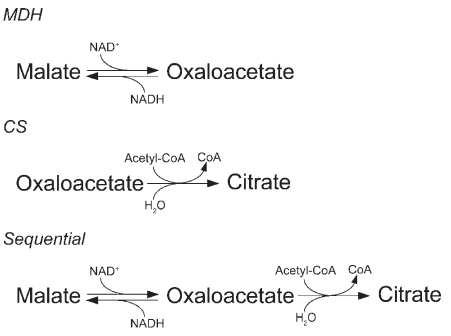

part of the tricarboxylic acid (TCA) cycle. MDH catalyzes the reversible conversion of malate to oxaloacetate using the cofactor NAD(H),[35] and CS carries out a Claisen condensation to catalyze the formation of citrate from oxaloacetate using acetyl-coenzyme A (acetyl-CoA).[36] Mitochondrial MDH and CS are found physically associated with each other in a multienzyme complex thought to enhance the overall kinetics of this pathway.[36−39] We used cytoplasmic MDH, which has been reported not to interact with CS, for the experiments described here in order to reduce protein−protein interactions.[40] Since we are relying on direct adsorption of the enzymes to the gold nanoparticles, differences in the relative affinity of the two enzymes for the particles (and any propensity for binding each other) will affect the bioconjugates formed.

Single-activity enzyme:Au NP (Au) bioconjugates will be described first, followed by those in which both CS and MDH were adsorbed to the same particles. The bioconjugates were named systematically based on the order in which enzymes were adsorbed to the nanoparticle surface (Scheme 1). Our notation lists the enzymes adsorbed from last to first, followed by the core Au separated by colons. For example, MDH:Au, CS:Au, and MDH/CS:Au were created using a single adsorption step while MDH:CS:Au was made by adsorbing MDH to a preexisting CS:Au bioconjugate. In all of the experiments described here, MDH has been fluorescently labeled with AlexaFluor 488 and CS with AlexaFluor 633.

MDH:Au and CS:Au Bioconjugates. Single-activity bioconjugates were formed through direct adsorption of either MDH or CS onto 30 nm Au NPs. Several ratios of enzyme to Au NP were tested to determine the effects of ratio on bioconjugate stoichiometry (i.e., the number of enzyme molecules adsorbed per particle) and enzyme activity.

Stoichiometry. We first determined the number of enzyme molecules adsorbed per particle as a function of the enzyme:Au ratio added to solution. After incubating enzymes with nanoparticles, the resulting bioconjugates were spun down, and any free enzyme remaining in solution was removed by rinsing. The Au cores of the bioconjugates were then dissolved in KCN solution, after which the released enzymes were quantified via fluorescence. This approach had been demonstrated previously for DNA oligonucleotide functionalized Au nanospheres[41] and for HRP:Au bioconjugates[21] and was extended here to the two-enzyme CS/MDH system by using a spectrally distinct dye on each enzyme (Alexa488 on MDH and Alexa633 on CS). We favor this method for determining the number of adsorbed enzymes over more common subtraction-based approaches because it enables us to account for any loss of Au NPs during rinsing due, e.g., to adsorption to the centrifuge tube walls, incomplete pelleting, and/or incomplete resuspension. Additionally, this approach is applicable regardless of the relative amounts of bound versus unbound enzyme; subtraction-based measurements are most accurate when the amount of adsorbed enzyme is a substantial fraction of the total. For the bioconjugates prepared here, the amount of adsorbed enzyme was generally 30% or more of the total enzyme, and subtraction gave comparable results to particle dissolution. Figure 1 compares these two quantification methods for each of the types of bioconjugates studied in this work. We used the values obtained from the direct measurement in our calculations throughout the paper.

Figure 2A shows our experimental results for enzyme:Au bioconjugate stoichiometry based on direct detection of fluorescently labeled MDH or CS. On the basis of crystal structure data,[42,43] we estimated that 73−106 MDH or 56−91 CS molecules would be required to form a monolayer on each 30.7-nm diameter Au NP, depending on adsorption orientation.[44] Because no effort was made to control adsorption orientation, we have assumed that enzymes adsorb randomly with an averaged molecular footprint in all estimations of how many layers a given number of enzyme molecules corresponds to (i.e., we assume a monolayer of MDH corresponds to roughly 90 molecules, and a monolayer of CS to ca. 74 molecules). Our data indicate that the Au NP did not become saturated at monolayer enzyme coverage, instead beginning to form multilayers at high enzyme:Au ratios. This type of adsorption behavior, including multilayer formation, has been observed for several other protein:Au bioconjugates,

(34) MDH (light spheres) and CS (dark spheres) were adsorbed either sequentially or simultaneously with Au nanoparticles. The amount of each enzyme measured for each bioconjugate is depicted as accurately as possible by estimating the number of layers of each enzyme present from their sizes. The diameter of each enzyme was determined by averaging measurements made in the x, y, and z dimensions of each enzymes crystal structure. This diameter was then used to calculate the area a single enzyme molecule would occupy on the surface area of the 30.7 nm diameter Au nanoparticle. The number of MDH or CS molecules necessary to cover the entire surface area of the nanoparticle was considered "monolayer coverage". To determine the number of MDH or CS necessary to form a complete layer on an existing MDH:Au or CS:Au bioconjugate, 2 times the average diameter of the previously immobilized enzyme was added to the diameter of the nanoparticle, and the surface area was recalculated. Note that, while some degree of enzyme unfolding is likely, we have not attempted to depict this in the scheme.

(35) Madern, D.; Ebel, C.; Mevarech, M.; Richard, S. B.; Pfister, C.; Zaccai, G. Insights into the molecular relationship between malate and lactate dehydrogenases: Structural and biochemical properties of monomeric and dimeric intermediates of a mutant of tetrameric L-[LDH-like] MDH from the halophilic archeon *Holorcula marismortui*. *Biochemistry* **2000**, *39*, 1001–1010.

(36) Kurz, L. C.; Drysdale, G.; Riley, M.; Tomar, M. A.; Chen, J.; Russell, R. J. M.; Danson, M. J. Kinetics and mechanism of the citrate synthase from Thermophilic archaeon *Thermoplasma acidophilum*. *Biochemistry* **2000**, *39*, 2283–2296.

(37) Koch-Schmidt, A.-C.; Mattiasson, B.; Mosbach, K. Aspects on microenvironmental compartmentation. *Eur. J. Biochem.* **1977**, *81*, 71–78.

(38) Tompa, P.; Batke, J.; Ovadi, J.; Welch, G. R.; Srere, P. A. Quantitation of the interaction between citrate synthase and malate dehydrogenase. *J. Bio. Chem.* **1987**, *262*, 6089–6092.

(39) Ovadi, J.; Srere, P. Metabolic consequences of enzyme interactions. *Cell Biochemistry and Function* **1996**, *14*, 249–258.

(40) Halper, L. A.; Srere, P. A. Interaction between citrate synthase and mitochondrial malate dehydrogenase in the presence of polyethylene glycol. *Arch. Biol. Biophys.* **1977**, *184*, 529–534.

(41) Demers, L. M.; Mirkin, C. A.; Mucic, R. C.; Reynolds, R. A., III; Letsinger, R. L.; Elghanian, R.; Viswanadham, G. A fluorescence-based method for determining the surface coverage and hybridization efficiency of thiol-capped oligonucleotides bound to gold thin films and nanoparticles. *Anal. Chem.* **2000**, *72*, 5535–5541.

(42) Chapman, A. D.; Cortes, A.; Dafforn, T. R.; Clarke, A. R.; Brady, R. L. Structural basis of substrate specificity in malate dehydrogenases: Crystal structure of a ternary complex of porcine cytoplasmic malate dehydrogenase, α-ketomalonate and tetrahydoNAD. *J. Mol. Biol.* **1999**, *285*, 703–712.

(43) Larson, S. B.; Day, J. S.; Nguyen, C.; Cudrey, R.; McPherson, A. Structure of pig heart citrate synthase at 1.78 anstrom resolution. *Acta Cryst. F* **2009**, *65*, 430–434.

(44) Considering the average diameter of the enzymes measured from crystal structures (6.5 nm diameter for MDH, 7.2 nm diameter for CS,[42,43] and the 30.7 nm diameter of Au), each MDH molecule would occupy at least 33 nm^2, and each CS molecule would occupy at least 40 nm^2 on the 2960 nm^2 surface area of Au.

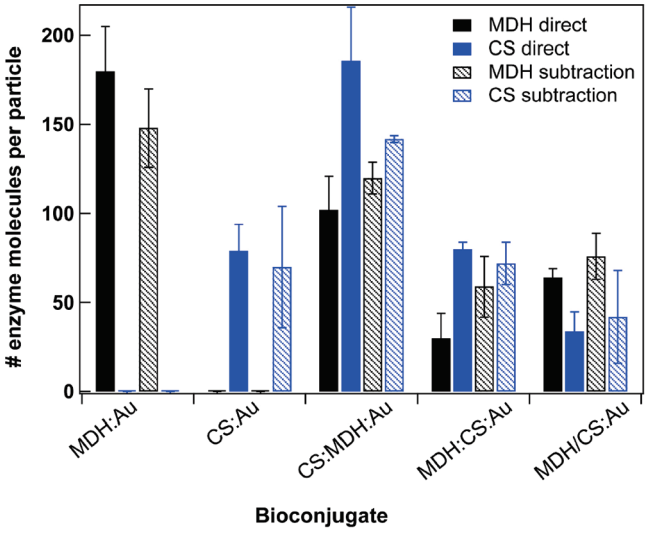

Figure 1. Comparison of two methods for quantifying the number of enzyme molecules bound to each Au NP. The "direct" method quantified fluorescently labeled proteins after removing unbound enzyme in the supernatant and dissolving the nanoparticle to release the bound enzyme. The "indirect" method quantified bound protein by measuring the unbound enzyme in solution and subtracting from the total enzyme added.

including protein A, concavalin A, bovine serum albumin, and HRP.[21,45,46]

At MDH:Au ratios of 100:1 and lower, nearly all the enzyme present adsorbed to the Au surface. At higher MDH:Au ratios, less than 60% of the total enzyme was associated with the bioconjugate. MDH:Au ratios of 100:1 or higher were also required to prevent salt-induced flocculation (Supporting Information, Figure 1). This is consistent with the ca. 90 molecules needed to form the first layer on the nanoparticle surface. Incubation of CS with Au also led to enzyme adsorption, with multilayer formation at high enzyme:Au ratios. In contrast to MDH:Au bioconjugates, however, a greater percentage of the CS added to solution remained unbound. At a solution ratio of 300:1, less than one-third of the CS molecules were associated with the nanparticles. CS also required greater concentrations to prevent salt-induced flocculation of the Au NPs as compared to MDH (Supporting Information, Figure 1). The lower affinity of CS for Au NPs as compared to MDH is consistent with their net charge at the adsorption pH and with their molecular weights. MDH (pI 10) is positively charged during adsorption, while the net charge on CS (pI 6−6.5) is negative.[47,48] The relationship between pI and adsorption pH is often invoked in attempts to control binding, but is complicated by the nonuniform spatial distribution of charged groups and by other types of adsorption interactions with the Au surface.[19,20,49] Using radiolabeled proteins, De Roe et al. found an inverse relationship between protein molecular weight and the amount of protein adsorbed per Au NP, suggesting

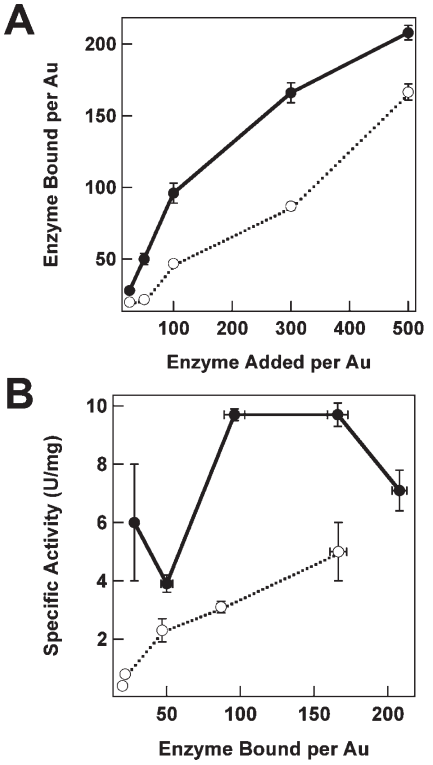

Figure 2. Single activity bioconjugate characterization. (**A**) The number of enzymes adsorbed per Au NP as a function of the ratio of enzyme:Au present in solution during conjugation of MDH (filled circles) and CS (open circles). (**B**) Specific activity of MDH (filled circles) and CS (open circles) as a function of the number bound.

that any specific surface interactions particular to a given protein were less important than the overall size of the adsorbing protein.[49]

Specific Activity. Adsorption of proteins to solid surfaces can lead to conformational changes[22−24] and/or reduced active site accessibility, decreasing the biological activity for the adsorbed proteins.[21,25,32] The effect of adsorption on activity varies with the identity of the enzyme, the type of solid support, and the way in which the enzymes are attached. For example, Gole et al.[32] found that fungal protease retained approximately 90% of its native activity upon adsorption to Au NPs, while Cans et al. determined that the specific activity of adsorbed HRP was as high as 50% that of native HRP with low surface coverages, but retained only 5% the native specific activity with higher surface coverages.[21] Even a lower retention of 1% native activity has been reported for lysozyme on silica particles.[50]

We quantified the activity of the adsorbed CS and MDH enzymes as compared to the same number of molecules free in solution (Table 1). MDH performs a reversible reaction to convert malate to oxaloacetate ($\nu_{m\text{-}o}$) or oxaloacetate to malate ($\nu_{o\text{-}m}$). The conversion of oxaloacetate to malate is more favorable and is routinely used in characterization of this enzyme;[51] however, the $\nu_{m\text{-}o}$ is relevant to its biological function in the citric acid cycle,[52] which includes the sequential reaction between MDH and CS studied here; hence, we performed activity assays for both reactions.

(45) Goodman, S. L.; Hodges, G. M.; Trejdosiewicz, L. K.; Livingston, D. C. Colloidal gold markers and probes for routine application in microscopy. *J. Microsc.* **1981**, *123*, 201–213.
(46) Warchol, J. B.; Brelinkska, R.; Herert, D. C. Analysis of colloidal gold methods for labeling proteins. *Histochemistry* **1982**, *76*, 567–575.
(47) Eanes, R. Z.; Kun, E. Separation and characterization of aconitate hydratase isoenzymes from pig tissues. *Biochim. Biophys. Acta* **1971**, *227*, 204–210.
(48) Kurz, L. C.; Shah, S.; Crane, B. R.; Donald, L. J.; Duckworth, H. W.; Drysdale, G. R. Proton uptake accompanies formation of the ternary complex of citrate synthase, oxaloacetate, and the transition-state analog inhibitor, carboxymethol-CoA. Evidence that a neutral enol is the activated form of acetyl-CoA in the citrate synthase reaction. *Biochemistry* **1992**, *31*, 7899–7907.
(49) De Roe, C.; Courtoy, P. J.; Baudhuin, P. A model of protein−colloidal gold interactions. *J. Histochem. Cytochem.* **1987**, *35*, 1191–1198.
(50) Bower, C. K.; Bothwell, M. K.; McGuire, J. Activity loss among T4 lysozyme charge variants after adsorption to colloidal silica. *Biotechnol. Bioeng.* **1999**, *64*, 373–376.
(51) Wilcock, A. R.; Goldberg, D. M. Kinetic determination of malate dehydrogenase activity eliminating problems due to spontaneous conversion of oxaloacetate to pyruvate. *Biochem. Med.* **1972**, *6*, 116–126.
(52) Srere, P. A.; Mattiasson, B.; Mosbach, K. An immobilized three-enzyme system: A model for microenvironmental compartmentation in mitochondria. *Proc. Natl. Acad. Sci. U.S.A.* **1973**, *70*, 2534–2538.

Table 1. Specific Activity of Free and Conjugated Enzymes Prepared at 300:1 Solution Enzyme:Au Ratio

	enzyme molecules per particle		MDH ($\nu_{m\text{-}o}$)		MDH ($\nu_{m\text{-}o}$)		CS	
sample	MDH	CS	U/mg	%	U/mg	%	U/mg	%
MDH	n.a.[a]	n.a.	182 ± 3	100	8.1 ± 0.6	100	n.a.	n.a.
MDH:Au	180 ± 25	n.a.	7 ± 3	4 ± 2	0.5 ± 0.2	8.1 ± 0.6	n.a.	n.a.
CS	n.a.	n.a.	n.a.	n.a.	n.a.	n.a.	73.6 ± 0.6	100
CS:Au	n.a.	79 ± 15	n.a.	n.a.	n.a.	n.a.	3.2 ± 0.3	4.3 ± 0.4
CS:MDH:Au	102 ± 19	186 ± 30	10 ± 2	5.5 ± 0.3	0.66 ± 0.05	6 ± 3	0.6 ± 0.2	0.8 ± 0.2
MDH:CS:Au	30 ± 14	80 ± 4	56 ± 15	31 ± 9	5.3 ± 0.4	65 ± 10	2.7 ± 0.2	3.7 ± 0.3
MDH/CS:Au	64 ± 5	34 ± 11	30 ± 6	16 ± 4	2.4 ± 0.3	30 ± 6	2.6 ± 0.7	4 ± 1

[a] Not applicable. Values for CS activity were not measured for MDH or MDH:Au, and values of MDH activity were not measured for CS or CS:Au.

Table 2. Kinetic Parameters for Bioconjugates

	MDH ($\nu_{o\text{-}m}$)		MDH ($\nu_{m\text{-}o}$)		CS	
sample	k_{cat} (s^{-1})	K_M (mM OAA)	k_{cat} (s^{-1})	K_M (mM malate)	k_{cat} (s^{-1})	K_M (μM OAA)
MDH	377 ± 46	0.020 ± 0.005	18 ± 4	0.3 ± 0.1	n.a.[a]	n.a.
MDH:Au	19 ± 5	0.04 ± 0.02	2.0 ± 0.3	0.18 ± 0.03	n.a.	n.a.
CS	n.a.	n.a.	n.a.	n.a.	26 ± 1	18 ± 5
CS:Au	n.a.	n.a.	n.a.	n.a.	7 ± 1	7.5 ± 0.4
CS:MDH:Au	119 ± 82	0.11 ± 0.09	1.8 ± 0.4	0.13 ± 0.03	0.28 ± 0.05	4 ± 1
MDH:CS:Au	642 ± 334	0.05 ± 0.02	12 ± 6	0.12 ± 0.02	1.9 ± 0.1	6 ± 2
MDH/CS:Au	37 ± 8	0.019 ± 0.009	4 ± 1	0.4 ± 0.2	3 ± 1	6 ± 2

[a] Not applicable. Values for CS activity were not measured for MDH or MDH:Au, and values of MDH activity were not measured for CS or CS:Au.

We also measured the rate of conversion of oxaloacetate to citrate for CS and determined specific activities for each enzyme from these data and the stoichiometry measurements described above.

Figure 2B shows the specific activity of adsorbed enzyme as a function of the amount of enzyme adsorbed per Au. For both MDH and CS, the specific activity of bound enzyme at all of the enzyme:Au ratios was greatly reduced as compared to free enzyme in solution. Specific activity for MDH:Au and CS:Au NP bioconjugates depended on the ratio of enzyme molecules to nanoparticles present in solution during adsorption. For CS:Au, when more enzyme was associated with the bioconjugate, the specific activity increased. For MDH:Au, the lowest enzyme:Au ratio was unstable, which led to large standard deviations in the specific activity; activities for 25 and 50 MDH per particle are not statistically different. The highest MDH:Au specific activities were found for intermediate enzyme:Au ratios. These results can be rationalized by considering that (a) submonolayer coverages may have allowed greater denaturation on the surface, and (b) multilayered assemblies could experience less conformational change but also limited substrate diffusion or steric hindrance due to neighboring enzyme molecules. These types of surface coverage-dependent changes in activity have been observed in other systems. For example, Aubin-Tam et al. found lower α-helical content for lower coverages of yeast cytochrome c bound to magnetic nanoparticles,[30] and Vertagel et al. found similar results for lysozyme on glass beads.[19] For multilayered enzyme assemblies, Cans et al. reported a similar trend with HRP−Au NP and linked it to decreased accessibility of the active site as the lateral packing of enzymes increases within a layer.[21]

K_M and k_{cat}. For further characterization, a solution ratio of 300:1 was used to prepare MDH:Au and CS:Au bioconjugates; this ratio was chosen because it was the lowest that provided bioconjugates stabilized from salt-induced flocculation (Supporting Information, Figure 1). The K_M, the substrate concentration at which half the active sites are filled, for free enzyme and MDH:Au and CS:Au are presented in Table 2.[53] The observed changes in K_M suggest differences in the secondary and tertiary structure of the enzyme[25,26] upon binding the particles. Such changes are expected. Pandey et al.[25] determined the K_M value for immobilized GOx on Au NPs to be slightly lower than that of the free enzyme, and similar results were found for lipase on Fe_3O_4 particles by Huang et al.,[29] where the K_M value was over 3 times lower for immobilized versus free enzyme. Jia et al.[56] also found a decrease in K_M value for immobilized α-chymotrypsin to 110 nm diameter particles. They also measured K_M as a function of scaffold size in the 100−1000 nm range, and found increasing K_M value with larger polystyrene bead sizes.

The turnover number, k_{cat}, is the number of substrate molecules converted to product per enzyme in a given amount of time.[33] For MDH:Au and CS:Au, the rate of substrate turnover is significantly diminished from that of free enzyme (Table 2), following the same trend as specific activity, which is not surprising considering the similarities between the measurements. These data complement the results seen for specific activity and K_M, representative of a change in the enzyme structure upon adsorption to Au NPs that decreases the catalytic ability of each enzyme.

Dual-Activity Bioconjugates. Having characterized the stoichiometry and kinetic parameters for MDH:Au and CS:Au bioconjugates, we next prepared dual-activity bioconjugates that contained both MDH and CS on the same nanoparticle (Scheme 1). MDH and CS were adsorbed either by incubating one of the enzymes with a preexisting bioconjugate of the other enzyme (e.g., MDH added to CS:Au to form MDH:CS:Au), or by simultaneous adsorption of both enzymes (MDH/CS:Au) as described in the Materials and Methods section. A solution ratio of 300:300:1 MDH:CS:Au was used in each case because it was the minimum ratio of each enzyme necessary to prevent flocculation in single-activity bioconjugates and provided the maximum specific activity of MDH:Au.

(53) While the specificity constant or catalytic efficiency (k_{cat}/K_M) can be calculated from the data presented in this section ,we have chosen to present the two values separately. Considering the effects of adsorption on enzyme structure and activity the differences between free and bound enzymes may limit the usefulness of the specificity constant for the bioconjugates presented here.[54,55]

(54) Eisenthal, R.; Danson, M. J.; Hough, D. W. Catalytic efficiency and k_{cat}/K_M: A useful comparator? *Trends in Biotechnol.* **2007**, *25*, 247−249.
(55) Fox, R. J.; Clay, M. D. Catalytic effectiveness, a measure of enzyme proficiency for industrial applications. *Trends in Biotechnol.* **2009**, *27*, 137–140.
(56) Jia, H.; Zhu, G.; Wang, P. Catalytic behaviors of enzymes attached to nanoparticles: The effect of particle mobility. *Biotechnol. And Bioengin.* **2003**, *84*, 406–414.

Stoichiometry. As for the single activity bioconjugates described above, the number of fluorescently labeled enzymes adsorbed per Au was determined for each of the three types of dual-activity bioconjugates (Table 1 and Figure 1). The three differed in the number of each enzyme adsorbed per particle.

CS:MDH:Au was made by adsorbing CS onto an existing MDH:Au bioconjugate. During the adsorption of CS, the amount of MDH adsorbed decreased from 180 ± 25 to 102 ± 19 per particle, consistent with loss of a second layer of MDH to leave behind roughly a monolayer of the enzyme. MDH loss was apparent not only in the reduced number of enzymes found associated with each particle, but also by the appearance of free MDH in the supernatant after centrifugation to remove the bioconjugates. Exchange between protein in solution and adsorbed protein has been observed previously for multilayers of BSA[57] and concavalin A.[45] The amount of CS in the CS:MDH:Au bioconjugates was much larger than in the single-activity CS:Au bioconjugates (186 ± 30 as compared with 79 ± 15). In part, this could be due to the larger diameter of the MDH-coated as compared to bare Au NPs requiring a greater number of CS molecules to coat this surface with a monolayer. However, it could indicate the formation of partial multilayers of CS and/or a change in the average CS adsorption orientation to yield a smaller molecular footprint.

MDH:CS:Au was made by adsorbing MDH to existing CS:Au bioconjugates; here the amount of CS present remained constant while MDH was adsorbed (79 ± 15 and 80 ± 4 for CS:Au and MDH:CS:Au, respectively). However, far less MDH adsorbed to the CS:Au bioconjugate than adsorbed directly to Au in the single-activity bioconjugate (30 ± 14 for MDH:CS:Au as compared with 180 ± 25 for MDH:Au). Thus, MDH cannot make multilayers on an underlying CS support, and most likely the amino acid residues involved in binding to CS-coated nanoparticles differ from those used in binding directly to the Au NP surface. Additionally, the fact that CS adsorbs to the MDH:Au bioconjugates in greater numbers than MDH adsorbs to the CS:Au bioconjugates suggests that the interacting portions of the enzymes are different in the two cases, either due to different orientations of adsorption or conformational changes that differ in the two cases.

When MDH and CS are adsorbed simultaneously (MDH/CS:Au), the resulting stoichiometry was unlike either of the sequentially formed bioconjugates. The amount of both MDH and CS adsorbed per particle was far lower, suggesting possible binding interactions in solution prior to the adsorption of either enzyme to the particles, and that the two enzymes adsorbed into a mixed arrangement on the Au surface. This correlates with the data presented in Figure 2, which shows that more MDH (70 kDa) molecules are adsorbed to Au than CS (85 kDa) using the same enzyme:Au ratios.

Specific Activity. Unlike the single-activity MDH:Au and CS:Au bioconjugates, several of the dual-activity bioconjugates exhibited greater than 10% of the specific activity seen for free MDH or CS in solution (Table 1), indicating that the enzyme conformation and/or environment in the these bioconjugates was more favorable than for the single-activity bioconjugates. For MDH the highest specific activity was found in MDH:CS:Au. The increase in specific activity over MDH:Au (10× for the forward reaction and 8× for the reverse reaction) is likely due to the fact that MDH was interacting with a layer of adsorbed CS instead of directly with the Au surface in the MDH:CS:Au. This is consistent with a greater retention of native conformation and/or a more favorable orientation of the MDH active site when it adsorbs atop the CS layer.

For CS the highest specific activity was found for CS:Au alone; this value decreased when MDH was adsorbed onto the CS:Au bioconjugate, but was still more active than CS:MDH:Au. These results suggest that the interaction between MDH and CS was detrimental to CS activity. Although we had selected the cytoplasmic MDH rather than the mitochondrial MDH in order to reduce binding interactions with the CS,[40] a computational study conducted at Virginia Tech[58] has predicted that CS also binds to cytoplasmic MDH. The model suggests the residues used are the same as those used in binding to mitochondrial MDH, but that the active site of cytoplasmic MDH is rotated away from the active site of CS, as compared to the alignment of the mitochondrial MDH and CS active sites.[58] In our experiments, this interaction could orient the CS active site away from solution, reducing the activity as compared to when the CS was adsorbed directly onto Au.

MDH activity in MDH/CS:Au was found to lie between that of MDH:CS:Au and CS:MDH:Au, consistent with the hypothesis that the enzyme adsorbs in multiple arrangements, both directly to Au and onto other adsorbed enzymes. CS activity was determined to be the same for MDH/CS:Au and MDH:CS:Au, suggesting that most of the CS present is adsorbed directly to Au.

For each enzyme reaction, MDH:CS:Au had the highest specific activity, suggesting that the structures of MDH and CS are less denatured and/or more favorably oriented in this arrangement than the other two multienzyme bioconjugates. Additionally, far less MDH adsorbs ($\ll$1 layer) to CS:Au than CS adsorbs (> 1 layer) to MDH:Au, which may allow for more interaction between solution and the bottom enzyme layer of MDH:CS:Au than CS:MDH:Au and increase activity of the bottom layer of enzyme.

K_M and k_{cat}. K_M and k_{cat} values for multiactivity bioconjugates are listed in Table 2. For MDH, the K_M for malate in MDH:CS:Au and CS:MDH:Au was lower than in MDH:Au or free MDH. For MDH/CS:Au, where the two enzymes are adsorbed simultaneously, the K_M was within error of the value for free MDH, suggesting that there is less change in the structure of the active site of MDH in this bioconjugate; this could be due to interactions between the two enzymes during the adsorption process. K_M determinations for MDH with oxaloacetate show a similar trend. The binding site affinity for MDH/CS:Au is equivalent to that of free MDH, suggesting little change in the structure of the active site upon adsorption. Comparison of the K_M values for CS:MDH:Au and MDH:CS:Au show that the K_M for oxaloacetate is closer to that of free MDH when it is adsorbed to a pre-existing bioconjugate; this may indicate less enzyme denaturation upon adsorption. For all three bioconjugates, the K_M of oxaloacetate for CS was approximately the same. Furthermore, the values were lower than that for free CS, indicating a change in active site structure. This suggests that adsorption to Au and MDH:Au affected the structure of CS to the same extent.

Similar to the trends found for specific activity, the turnover number for MDH is higher when adsorbed to existing CS:Au bioconjugates. For MDH, $\nu_{m\text{-}o}$ is at least 6 times and $\nu_{o\text{-}m}$ is 30 times faster than MDH:Au; this increase is due to the interaction between MDH and CS, which is less destructive to MDH activity than

(57) Xie, H.; Tkachenko, A. G.; Glomm, W. R.; Ryan, J. A.; Brennaman, M. K.; Papanikolas, J. M.; Franzen, S.; Feldheim, D. L. Critical flocculation concentrations, binding isotherms, and ligand exchange properties of peptide-modified gold nanoparticles studied by UV-visible, fluorescence, and time-correlated single photon counting spectroscopies. *Anal. Chem.* **2003**, *75*, 5797–5805.

(58) Burbulis, I. E. Macromolecular organization of flavonoid biosynthesis in *Arabidopsis thaliana*. Ph.D. Dissertation, Virginia Polytechnic Institute and State University, Blacksburg, VA, 1998.

Table 3. Activity per Particle

	MDH ($\nu_{o\text{-}m}$) ($\times 10^{-14}$ U/Au)	MDH ($\nu_{o\text{-}m}$) ($\times 10^{-14}$ U/Au)	CS ($\times 10^{-14}$ U/Au)	sequential ($\times 10^{-14}$ U/Au)
MDH:Au	16 ± 6	1.1 ± 0.4		
CS:Au			3.6 ± 0.3	
CS:MDH:Au	21 ± 4	1.4 ± 0.1	0.9 ± 0.3	0.5 ± 0.1
MDH:CS:Au	20 ± 5	1.9 ± 0.1	3.1 ± 0.2	1.7 ± 0.2
MDH/CS:Au	22 ± 4	1.8 ± 0.2	1.2 ± 0.3	0.18 ± 0.03

the interaction of MDH with Au NP based on enzyme activity. For $\nu_{o\text{-}m}$, the turnover rate is 1.7 times the rate for free enzyme; however, due to the large standard deviation in $\nu_{o\text{-}m}$ for the MDH:CS:Au, the two values are not statistically different according to a student's t test. Rate enhancements have been seen before for bioconjugates and are usually reported as V_{max} (equal to $k_{cat} \times E_{total}$). For example, Huang et al. found that lipase immobilized to magnetic nanoparticles had a greater V_{max} than free lipase,[29] while Pandey et al. found that immobilized GOx was an order of magnitude more active than free GOx.[25] Both sets of authors attributed this increase to structural changes in the enzyme upon adsorption that allowed for a better orientation of the active site. In the case of MDH:CS:Au, the interaction between MDH and CS may have a similar effect on active site orientation.

Similarly the turnover number for CS was greater for MDH:CS:Au than CS:MDH:Au, suggesting that there is a more favorable interaction between CS and Au than MDH:Au. As seen in Table 1, there is less MDH present than necessary to form a monolayer, increasing the likelihood of substrate diffusing to the CS active site. This corresponds with K_M data (Table 2), where the substrate specificity was greater for CS adsorbed to Au than CS adsorbed to MDH:Au. Again, this could be due to a specific interaction between MDH and CS causing an unfavorable orientation of CS when it adsorbs.[58]

For MDH/CS:Au the MDH k_{cat} of each reaction was approximately 2 times greater than that for MDH:Au, suggesting that coimmobilization led to less denaturation than when adsorbed directly to Au NPs, but the turnover number for each reaction was lower than MDH:CS:Au. The CS turnover rate was lower for MDH/CS:Au than CS:Au. Taken together, these data imply that the active sites for some of the MDH and CS molecules were blocked by other enzymes in this mixed arrangement.

This data suggests that both enzymes interact with the Au surface in similar ways to the first enzyme adsorbed in the sequential adsorption bioconjugates. K_M data for this bioconjugate indicate that MDH is in a near native conformation, while specific activity and turnover number suggest that catalysis may be limited by the surrounding adsorbed enzyme.

Activity per Particle. An important measure for characterizing enzyme bioconjugates is activity per particle, which is often easier to determine than specific activity for the adsorbed enzymes and is relevant for biotechnological applications. High enzymatic activities on a per particle basis can result from a large number of moderately active molecules on each particle or a smaller number of highly active molecules. In previous reports, the per particle activity has been used to show the increased stability of adsorbed enzymes over time and to increased pH;[26,27] here we report activity per particle (Table 3) to compare the catalytic ability of the different bioconjugates produced. We found similar trends in the activity per Au as for specific activity (Table 1). Interestingly, the reverse MDH reaction was consistent and independent of the type of bioconjugate, indicating that the large number of enzymes adsorbed was able to offset the effect of enzyme denaturation. This underscores the idea that activity measurements without knowledge of the amount of enzyme present are incomplete and cannot speak to the amount of enzyme denaturation.

Sequential Activity. Because the product of MDH (oxaloacetate) is a substrate for CS, it is also possible to evaluate the overall activity of the dual enzyme bioconjugates for conversion of malate to citrate. Sequential activity of MDH and CS in multiactivity bioconjugates was measured as activity per particle (Table 3). The highest sequential activity of MDH and CS was found for MDH:CS:Au. Examination of the individual activity per Au rates indicates that the individual reaction rates are limiting factors for CS:MDH:Au (CS rate) and MDH:CS:Au (MDH rate) but not for MDH/CS:Au. For MDH:CS:Au, the sequential rate of reaction is very close to the rate of oxaloacetate production by MDH, suggesting that the intermediate is efficiently transferred from MDH to CS. For CS:MDH:Au, the rate of oxaloacetate production by MDH is faster than the rate of consumption by CS; this allows oxaloacetate time to build up or diffuse away from the bioconjugate, leading to a less efficient reaction. The individual MDH and CS rates per particle are 10 times faster than the rate of the sequential reaction, which may be due to inefficient diffusion of oxaloacetate from the MDH active site to the CS active site. These data suggest that the organization and ratio of activity of sequential enzymes is important for the sequential rate of reaction.

Previous reports have found that the rate of sequential activity for a multiple enzyme system is improved by colocalization. For example, Watanabe and Ishihara found that a higher local concentration of each enzyme lead to higher sequential activity rates when a three-enzyme system was immobilized to polymer nanoparticles, due to effective diffusion of intermediates.[9] Similar results were reported by Pescador et al. for layer-by-layer (LbL) assemblies of GOx and HRP.[8] Pescador et al.[8] also found that an optimized configuration of GOx and HRP in LbL assemblies lead to a 2.5-fold increase in the sequential reaction rate. Here, the individual MDH (forward reaction) and CS rates are nearly an order of magnitude faster than the sequential reaction rate, suggesting that reaction is limited instead by an inability for the intermediate, oxaloacetate, to diffuse from one active site to the other efficiently.

Conclusions

The work presented here demonstrates how activity measurements combined with detailed knowledge of bioconjugate stoichiometry can be used to further the characterization of enzyme adsorbed to nanoparticulate surfaces. In particular, it can be noted that (1) MDH adsorbed to CS:Au bioconjugates has superior kinetic parameters and ability to catalyze substrate as compared to CS adsorbed to MDH:Au and more closely approaches the characteristics of free enzyme. Additionally, CS orientation when adsorbed to MDH:Au appears to be dictated by a specific protein−protein interaction. While every set of enzymes will behave differently, this suggests that near-native activity and/or specific orientation on a particle can be achieved with a direct adsorption strategy even for proteins not known for strong binding in solution. (2) Kinetic characterization can be used to help understand how multiple types of enzymes are adsorbed single nanoparticle and the effect on each enzyme's structure and activity. Furthermore, common measurements of activity without knowledge of stoichiometry may be misleading when comparing methods for bioconjugate formation since the number of enzymes present can obscure differences in activity. (3) The sequential activity of two types of enzymes adsorbed to the same nanoparticle is dependent not only on the individual reaction rates, but also on the ability of intermediates to move between active sites. Although the bioconjugates

described here differ substantially from the enzyme complexes found in biological cells, multienzyme complexes are known to form intracellularly.[37,39,59] Our findings underscore the importance of control over enzyme position—here determined by addition order—in biological or artificial multienzyme complexes to enable effective transfer of intermediates between active sites.

Materials and Methods

Materials. Colloidal gold particles (mean diameter 30.7 nm, 2×10^{11} particles/mL) were purchased from Ted Pella, Inc. (Redding, CA). AlexaFluor 488 and AlexaFluor 633 protein labeling kits were purchased from Invitrogen (Carlsbad, CA). CS from porcine heart (EC 2.3.3.1) ammonium sulfate suspension, MDH from porcine heart (EC 1.1.1.37) ammonium sulfate suspension solution, L-(−)-malic acid, oxaloacetic acid, acetyl coenzyme A trilithium salt, β-nicotinamide adenine dinucleotide hydrate (NAD^+), β-nicotinamide adenine dinucleotide reduced disodium salt hydrate (NADH), Trisma hydrochloride (Tris[hydroxymethyl]aminomethane hydrochloride), Trisma base (Tris[hydroxymethyl]aminomethane), sodium bicarbonate, and Ellman's Reagent (5,5′-dithiobis[2-nitrobenzoic acid]) (DTNB) were purchased from Sigma-Aldrich (St. Louis, MO). Pall Life Sciences Nanosep 10k MWCO centrifugal devices and Whatman 20 nm pore diameter syringe filters were purchased from VWR. Deionized water with a resistivity of ≥ 18.2 MΩ from a Barnstead NANOpure Diamond water purification system (Van Nuys, CA) was used in all experiments.

Enzyme Labeling. A 10 kDa MWCO centrifuge filter was used to remove ammonium sulfate, which can reduce labeling efficiency by outcompeting primary amines in the protein structure for the coupling reaction. CS and MDH were resuspended in 5 mM sodium bicarbonate (pH 8.3) at a 2 mg/mL concentration prior to fluorescent labeling. CS and MDH were labeled with AlexaFluor 633 and AlexaFluor 488 respectively, according to the protocol provided by Invitrogen.

Flocculation Assays. Flocculation assays are a traditional means of determining how much protein must be added to produce a stable bioconjugate with gold nanoparticles.[2,45,49] The Au NPs used in bioconjugation are negatively charged, and prevented from aggregating by electrostatic repulsions. Addition of NaCl to screen these electrostatic repulsions results in aggregation or flocculation, which is observable as a color change from red to blue or purple. Adsorption of protein to the nanoparticle surface creates a steric barrier that prevents salt-induced flocculation.[2] Here, we performed flocculation assays to determine the minimum amount of fluorescently labeled CS or MDH necessary to prevent single enzyme bioconjugates from salt-induced aggregation.[2] Samples with mole ratios of enzyme:Au of 25:1 to 500:1 were prepared by diluting Au particles (3.75×10^{-14} mol) in buffer then adding enzyme from stock prepared in 5 mM sodium bicarbonate (pH 10) for a total volume of 150 μL. Samples were incubated for 1 h at room temperature protected from light followed by addition of 150 μL of buffer to dilute the solution for absorbance measurements and 17 μL of 2 M NaCl, to induce aggregation of unprotected nanoparticles. After 60 min, incubation samples were analyzed by absorbance spectroscopy using a Hewlett-Packard 8453 diode-array UV−visible spectrometer with Agilent ChemStation Software.

Enzyme Conjugation and Bioconjugate Purification. Single enzyme bioconjugates were prepared by first concentrating 6.0×10^{11} Au NPs (9.96×10^{-13} mol) to a volume of 1 mL and washing with 5 mM sodium bicarbonate (pH 8.3) in 20 nm filtered water to remove any possible contaminants. CS or MDH was then added from a stock solution in the same buffer to create the desired enzyme:Au ratio, and buffer was added to a final volume of 1.5 mL. Enzymes were allowed to adsorb to the surface of the nanoparticle for 1 h at 4 °C protected from light. Excess enzyme was subsequently removed by centrifugation of the bioconjugates at 5000*g* for 15 min at 4 °C, the supernatant was removed, and bioconjugates were resuspended in 1.5 mL of fresh buffer. This process was repeated three times to ensure all excess enzyme was removed from the bioconjugate solution. Multienzyme bioconjugates were prepared by adsorbing CS and MDH to the surface of the same nanoparticle either sequentially or simultaneously (Scheme 1). Bioconjugates were formed in sequential steps by adsorbing CS or MDH onto the surface of a preexisting bioconjugate containing the other enzyme, or by simultaneously adding both enzymes to bare Au NPs. All incubation and washing procedures follow those laid out for single enzyme bioconjugates.

Enzyme Activity Assays. To measure the rate of reaction for the conversion of malate to oxaloacetate ($\nu_{m\text{-}o}$) for MDH in single and multienzyme bioconjugates of 100 mM Tris (pH 8.1), 25 μL of 36 mM malate and 25 μL of 60 mM NAD^+ (25 μL of 60 mM oxaloacetate and 25 μL of 12 mM NADH for the conversion of oxaloacetate to malate by MDH or $\nu_{o\text{-}m}$), for a final concentration of 0.3 mM malate and 0.1 mM NAD^+ (0.5 mM oxaloacetate and 0.1 mM NADH), were mixed in a cuvette and equilibrated to room temperature, in accordance with previous reports.[52] A volume of 200 μL of bioconjugate was then added to the solution, which was mixed again to ensure homogeneity, and the absorbance of NADH was monitored at 340 nm for 5 min (Scheme 2) $\varepsilon = 6220\ M^{-1}\ cm^{-1}$.[60] For each assay, the volume of bioconjugate added (200 μL) remained constant and the concentration of bioconjugate was measured by the absorbance of the gold plasmon at 524 nm ($\varepsilon = 3.585 \times 10^9\ M^{-1}\ cm^{-1}$).[61] Each assay was repeated at least three times and had a total volume of 3 mL. The activity of CS for conversion of oxaloacetate to citrate ($\nu_{o\text{-}c}$) in single and multienzyme bioconjugates was assayed in similar fashion to MDH with the exception that 25 μL of 12 mM acetyl-CoA and 25 μL of 60 mM oxaloacetate were used as substrates with 25 μL of 18 mM DTNB, for a final concentration of 0.5 mM oxaloacetate, 0.1 mM acetyl-CoA, and 0.15 mM DTNB. DTNB was added to monitor the production of coenzyme A by CS by adsorption at 412 nm $\varepsilon = 13{,}600\ M^{-1}\ cm^{-1}$.[62,63]

Determination of kinetic constants was carried out in the same fashion, varying the amount of either malate or oxaloacetate while the concentration of the conenzymes remained constant. K_M, V_{max}, and k_{cat} were determined by nonlinear regression of the Michaelis−Menten equation[33] using eq 1 for CS and the forward reaction of MDH, and eq 2 for the reverse reaction of MDH; this was necessary because high concentrations of oxaloacetate are known to inhibit MDH activity.[64,65]

$$v = \frac{V_{max}[S]}{K_M + [S]} \quad (1)$$

$$v = \frac{V_{max}[S]}{[S] + K_M(1 + S/k_i)} \quad (2)$$

Sequential activity of MDH and CS in multienzyme bioconjugates was measured by monitoring the production of coenzyme A

(59) (a) Ovadi, J.; Srere, P. A. Macromolecular compartmentation and channeling. *Int. Rev. Cytol.* **2000**, *192*, 255–280. (b) Srere, P. A. Complexes of sequential metabolic enzymes. *Annu. Rev. Biochem.* **1987**, *56*, 89–124.

(60) Dawson, R. B. *Data for Biochemical Research*, 3rd ed.; Clarendon Press: Oxford, 1985; p 122.

(61) Ted Pella, Inc. www.tedpella.com (accessed May 2010).

(62) Santoro, N.; Brtva, T.; Vander Roest, S.; Siegel, K.; Waldrop, G. L. A high-throughput screening assay for the carboxyltransferase subunit of acetyl-CoA carboxylase. *Anal. Biochem.* **2006**, *354*, 70–77.

(63) Jansen, H.; Hulsmann, W. C. Long-chain acyl-CoA hydrolase activity in serum: identity with clearing factor lipase. *Biochim. Biophys. Acta* **1973**, *296*, 241–248.

(64) Wang, J.; Araki, T.; Ogawa, T.; Matsuoka, M.; Fukuda, H. A method of graphically analyzing substrate-inhibition kinetics. *Biotechnol. Bioeng.* **1999**, *62*, 402–411.

(65) Lindbladh, C.; Rault, M.; Haggland, C.; Small, W. C.; Mosbach, K.; Buelow, L.; Evans, C.; Srere, P. A. Preparation and kinetic characterization of a fusion protein of yeast mitochondrial citrate synthase and malate dehydrogenase. *Biochemistry* **1994**, *33*, 11692–11698.

in the presence of 25 μL of 36 mM malate, 25 μL of 60 mM NAD^+, 25 μL of 12 mM acetyl-CoA, and 25 μL of DTNB in a total volume of 3 mL, for a final substrate concentration of 0.3 mM malate, 0.5 mM NAD^+, and 0.1 mM acetyl-CoA, with 0.15 mM DTNB to monitor CoA production.[36] Kinetic assays were run for 300 s time periods with a full spectrum collected every 30 s.

Determination of Enzyme:Nanoparticle Stoichiometry. The number of enzymes adsorbed per nanoparticle was determined by two complementary methods: (1) indirectly, by monitoring the enzyme remaining in solution after conjugation to the nanoparticles. The concentration of enzyme found in solution after conjugation was subtracted from the initial enzyme concentration and divided by the initial Au concentration; measurements of enzyme concentration were corrected to account for enzyme lost to adsorption to the ependorf tube.[21] (2) Directly, by washing away excess enzyme and dissolving the Au core to release the adsorbed enzymes into solution for quantification. This was done by first determining the concentration of bioconjugates based on the absorbance of the gold nanoparticles at 524 nm, $\varepsilon = 3.585 \times 10^9\ M^{-1}\ cm^{-1}$.[61] One hundred microliters of 50 mM potassium cyanide was then added to 100 μL of bioconjugate, mixed, and allowed to react for 12 h at 4 °C. A Horiba Jobin Yvon Fluorolog 3-21 was then used to find the concentration of each fluorescently labeled enzyme in solution. Stoichiometry is expressed as the ratio of enzyme to Au present after conjugation and washing steps.

Acknowledgment. This work was supported by the National Institutes of Health, Grant R01GM078352, and by the National Science Foundation, Grant CHE-0750196, cofunded by the MCB Division.

Supporting Information Available: Flocculation data for MDH and CS adsorption to Au NPs. This information is available free of charge via the Internet at http://pubs.acs.org/.